J. Phys. B: At. Mol. Opt. Phys. **41** (2008) 155201 (10pp) doi:10.1088/0953-4075/41/15/155201

Low and intermediate energy electron collisions with the C_2^- molecular anion

Gabriela Halmová[1], J D Gorfinkiel[2] and Jonathan Tennyson[1]

[1] Department of Physics and Astronomy, University College London, Gower St, London WC1E 6BT, UK
[2] Department of Physics and Astronomy, The Open University, Walton Hall, MK7 6AA Milton Keynes, UK

Received 4 May 2008, in final form 9 June 2008
Published 18 July 2008
Online at stacks.iop.org/JPhysB/41/155201

Abstract
Calculations are presented which use the molecular *R*-matrix with pseudo-states (MRMPS) method to treat electron impact electron detachment and electronic excitation of the carbon dimer anion. Resonances are found above the ionization threshold of C_2^- with $^1\Sigma_g^+$, $^1\Pi_g$ and $^3\Pi_g$ symmetry. These are shape resonances trapped by the effect of an attractive polarization potential competing with a repulsive Coulomb interaction. The Π_g resonances are found to give structure in the detachment cross section similar to that observed experimentally. Both excitation and detachment cross sections are found to be dominated by large impact parameter collisions whose contribution is modelled using the Born approximation.

(Some figures in this article are in colour only in the electronic version)

1. Introduction

The carbon dimer anion is unusual among small anions in having bound electronically excited states. In addition electron scattering experiments performed in storage rings showed that C_2^- was one of a number of diatomic anions which, at least temporarily, are able to bind an additional electron leading to pronounced resonance structures in their measured cross sections (Andersen *et al* 1996, 2001b, Pedersen *et al* 1998, 1999, Collins *et al* 2005). Similar results have also been found for systems containing the NO_2^- anion (Andersen *et al* 2001a, Svendsen *et al* 2005). Given that the electron collisions occur against the background of a strongly repulsive Coulomb interaction, the occurrence of such resonance structures, which generally lie above the threshold for electron impact detachment, was unanticipated.

Theoretically the treatment of electron collisions with these diatomic anions is complicated by the need to treat the region immediately above the electron detachment threshold. Such intermediate energy calculations are difficult because of the presence of two continuum electrons. Previous theoretical studies have used bound state methods either unadapted (Pedersen *et al* 1999) or with an absorbing potential (Sommerfeld *et al* 1997, 2000) to study the continuum states of C_2^{2-}.

In a preliminary publication (Halmová and Tennyson 2008) we reported calculations using the molecular *R*-matrix with pseudo-states (MRMPS) method (Gorfinkiel and Tennyson 2004, 2005) which found a number of low-lying resonances. In this work we report fully on these calculations, including details of the models we tested to produce stable calculations and to demonstrate that our results are robust. In addition we report results for electron impact excitation of C_2^-.

2. Method

The *R*-matrix method is based on dividing coordinate space into two regions using a spherical boundary of radius *a* centred on the centre of mass of the target molecule (Burke and Berrington 1993, Burke and Tennyson 2005). The radius of the boundary is chosen so that the inner region contains all the electronic cloud of the target molecular states included in the calculation.

Inside the *R*-matrix sphere it is necessary to consider all short-range interactions between the *N* target electrons and the scattering one, such as exchange and electron correlation. In the outer region these effects are negligible so the scattering electron can be described as moving in the long-range multipole potential of the target molecule.

The accuracy of this method is strongly dependent on the representation of the problem in the inner region

(Tennyson 1996b). In standard, low-energy calculations, the wavefunction for an N+1 electrons system in the inner region is given by the expansion

$$\psi_k^{N+1} = \mathcal{A}\sum_{ij} a_{ijk}\Phi_i(\mathbf{x}_1 \ldots \mathbf{x}_N)u_{ij}(\mathbf{x}_{N+1}) + \sum_i b_{ik}\chi_i(\mathbf{x}_1 \ldots \mathbf{x}_{N+1}) , \quad (1)$$

where k represents the kth solution of the inner region Hamiltonian, $\mathcal{A}$ is the antisymmetrization operator, $\mathbf{x}_i$ are the spatial and spin coordinates of electron i, u_{ij} are continuum orbitals (COs) which represent the scattering electron (Tennyson and Morgan 1999), a_{ijk} and b_{ik} are variational coefficients, Φ_i is the wavefunction of the ith target state and χ_i are L^2 functions constructed from the target occupied and virtual molecular orbitals. These functions represent electron correlation and polarization effects. In the first sum, the configuration state functions are constrained to give the correct (target) space and spin symmetry for the first N-electrons as well as the correct total, N+1 electron space–spin symmetry. Doing this requires special consideration of phase effects due to electron ordering in the wavefunction (Tennyson 1997).

In the standard formulation of the R-matrix method all the solutions of the inner region problem are required to construct the R-matrix on the boundary (Burke and Berrington 1993). This presents a serious computational barrier for large calculations as diagonalizing the entire Hamiltonian may not be feasible. For some of the calculations discussed below we used the partitioned R-matrix method (Tennyson 2004), which only requires the low-lying eigenvalues and which has been demonstrated to give good results for the electron–C_2^- problem (Tennyson and Halmová 2007).

Here we use the UK polyatomic R-matrix code (Morgan *et al* 1997) rather than the specialized, Slater orbital-based diatomic code. This is because the MRMPS method described below relies on the use of Gaussian-type orbitals (GTOs) and is therefore only implemented in this code. The highest symmetry available in the polyatomic code is D_{2h} which is a subgroup of the true $D_{\infty h}$ symmetry of C_2^-. All calculations presented here were performed in D_{2h} symmetry. In the polyatomic suite target, continuum and MRMPS pseudo-continuum orbitals are all represented by a linear combination of GTOs. The target wavefunctions are expanded as a linear combination of the configurations ϕ_k:

$$\Phi_i(\mathbf{x}_1 \ldots \mathbf{x}_N) = \sum_k c_{ik}\phi_k(\mathbf{x}_1 \ldots \mathbf{x}_N) , \quad (2)$$

where the c_{ik} coefficients are determined by diagonalizing the Hamiltonian of the molecular target. The quality of the target wavefunctions is dependent on the size of this expansion, as is indirectly, the quality of the scattering calculation (Tennyson 1996b).

The central idea of the MRMPS method is the augmentation of the close-coupling expansion (1) with extra 'target' wavefunctions Φ_i that represent pseudo-states. Unlike the usual target wavefunctions, these pseudo-states are not approximations to true eigenstates of the target, but are used to represent a discretized version of the electronic continuum. These pseudo-states are obtained by diagonalizing the target electronic Hamiltonian expressed in an appropriate basis of configurations, see below.

As we are considering an anionic target, there is a finite number of bound target electronic states: three in the case C_2^-. This means that, unlike previous MRMPS studies (Gorfinkiel and Tennyson 2004, 2005), the pseudo-states are expected to all lie above the threshold to ionization (electron detachment) where they represent the discretized target continuum. Of course, as the pseudo-continuum orbitals are added to the target basis they also influence the representation of the target states. It is a standard and tested assumption of the R-matrix with pseudo-states method that electron impact ionization cross sections can be obtained by summing the cross sections for excitation of pseudo-states which lie above the vertical excitation threshold (Bartschat and Bray 1996).

To generate configurations that describe an ionized target, the MRMPS method uses an extra set of orbitals called pseudo-continuum orbitals (PCOs). These orbitals are used to describe the ionized electron. The PCOs are expanded in terms of an even-tempered basis set (Schmidt and Ruedenberg 1979) of GTOs centred at the centre of mass of the system. In this type of basis set, the exponents of the GTOs follow:

$$\alpha_i = \alpha_0\beta^{(i-1)}, \qquad \beta > 1, \qquad i = 1, \ldots, L , \quad (3)$$

where by choosing different values of the parameters α_0 and β different basis sets can be systematically generated. This is useful for checking the convergence and stability of the calculation and, of particular importance here, identifying physical resonances as distinct from the pseudo-resonances which are a known artefact of the RMPS procedure (Bartschat *et al* 1996).

Given that the COs are also represented by GTOs, to avoid problems with linear dependence it is necessary to remove those CO basis functions from the set whose exponents are greater than α_0. Even after this condition care has to be taken to ensure that the three basis sets (target, CO and PCO) give a linearly independent set of orbitals. To do this the PCOs are first Schmidt orthogonalized to the target molecular orbitals (MOs) and then symmetric orthogonalized among themselves. At this stage those orbitals with eigenvalues of the overlap matrix less than a deletion threshold δ, here taken as 4×10^{-6}, were assumed to be linearly dependent and were removed from the basis. This procedure is repeated for the COs, here using $\delta = 2 \times 10^{-6}$.

3. Calculations

3.1. Target representation

The starting point for the present calculations was our previous study of the electron–C_2 system (Halmová *et al* 2006). The ground-state Hartree–Fock configuration of C_2 is $1\sigma_g^2\,1\sigma_u^2\,2\sigma_g^2\,2\sigma_u^2\,1\pi_u^4$ while for C_2^- the extra electron is in the $3\sigma_g$ orbital. In that work the states of C_2 were represented using the double-zeta plus polarization (DZP) Gaussian basis set of Dunning (1970), natural orbitals and a complete active space configuration interaction (CAS-CI) in which the four

Table 1. Configurations used in the various target models tested. N is the size of the resulting Hamiltonian matrix for ^2A_g symmetry and PCO means pseudo-continuum orbital.

Model	N	Configurations
1	1110	$(1\sigma_g\,1\sigma_u)^4\,(2\sigma_g\,3\sigma_g\,4\sigma_g\,2\sigma_u\,3\sigma_u\,1\pi_u\,1\pi_g)^9$
		$(1\sigma_g\,2\sigma_g\,1\sigma_u\,2\sigma_u\,1\pi_u)^{12}\,(\text{PCOs})^1$
2	140	$(1\sigma_g\,2\sigma_g\,1\sigma_u\,2\sigma_u)^8\,1\pi_u{}^4\,(3\sigma_g\,3\sigma_u\,1\pi_g)^1$
		$(1\sigma_g\,2\sigma_g\,1\sigma_u\,2\sigma_u)^8\,1\pi_u{}^3\,(3\sigma_g\,3\sigma_u\,1\pi_g)^2$
		$(1\sigma_g\,2\sigma_g\,1\sigma_u\,2\sigma_u)^8\,1\pi_u{}^4\,(\text{PCOs})^1$
		$(1\sigma_g\,2\sigma_g\,1\sigma_u\,2\sigma_u)^8\,1\pi_u{}^3\,(3\sigma_g\,3\sigma_u\,1\pi_g)^1\,(\text{PCOs})^1$
3	1600	$(1\sigma_g\,1\sigma_u\,2\sigma_g)^6\,1\pi_u{}^4\,(2\sigma_u\,3\sigma_g\,3\sigma_u\,1\pi_g)^3$
		$(1\sigma_g\,1\sigma_u\,2\sigma_g)^6\,1\pi_u{}^3\,(2\sigma_u\,3\sigma_g\,3\sigma_u\,1\pi_g)^4$
		$(1\sigma_g\,1\sigma_u\,2\sigma_g)^6\,1\pi_u{}^4\,(2\sigma_u\,3\sigma_g\,3\sigma_u\,1\pi_g)^2\,(\text{PCOs})^1$
		$(1\sigma_g\,1\sigma_u\,2\sigma_g)^6\,1\pi_u{}^3\,(2\sigma_u\,3\sigma_g\,3\sigma_u\,1\pi_g)^3\,(\text{PCOs})^1$
4	425	$(1\sigma_g\,1\sigma_u)^4\,(2\sigma_g\,3\sigma_g\,2\sigma_u\,3\sigma_u\,1\pi_u\,1\pi_g)^9$
		$(1\sigma_g\,2\sigma_g\,1\sigma_u\,2\sigma_u)^8\,1\pi_u{}^4\,(\text{PCOs})^1$
		$(1\sigma_g\,2\sigma_g\,1\sigma_u\,2\sigma_u)^8\,1\pi_u{}^3\,(3\sigma_g\,3\sigma_u\,1\pi_g)^1\,(\text{PCOs})^1$
5	597	$(1\sigma_g\,1\sigma_u)^4\,(2\sigma_g\,3\sigma_g\,2\sigma_u\,3\sigma_u\,1\pi_u\,1\pi_g)^9$
		$(1\sigma_g\,1\sigma_u)^4\,(2\sigma_g\,2\sigma_u\,1\pi_u)^8\,(\text{PCOs})^1$
		$(1\sigma_g\,1\sigma_u)^4\,(2\sigma_g\,2\sigma_u\,1\pi_u)^7\,(3\sigma_g\,3\sigma_u\,1\pi_g)^1\,(\text{PCOs})^1$
6	3111	$(1\sigma_g\,1\sigma_u)^4\,(2\sigma_g\,3\sigma_g\,2\sigma_u\,3\sigma_u\,1\pi_u\,1\pi_g)^9$
		$(1\sigma_g\,1\sigma_u)^4\,(2\sigma_g\,2\sigma_u\,1\pi_u)^8\,(\text{PCOs})^1$
		$(1\sigma_g\,1\sigma_u)^4\,(2\sigma_g\,2\sigma_u\,1\pi_u)^7\,(3\sigma_g\,3\sigma_u\,1\pi_g)^1\,(\text{PCOs})^1$
		$(1\sigma_g\,1\sigma_u)^4\,(2\sigma_g\,2\sigma_u\,1\pi_u)^6\,(3\sigma_g\,3\sigma_u\,1\pi_g)^2\,(\text{PCOs})^1$
7	20 454	$(1\sigma_g\,1\sigma_u\,2\sigma_g)^6\,(2\sigma_u\,3\sigma_g\,3\sigma_u\,1\pi_g\,1\pi_u)^7$
		$(1\sigma_g\,1\sigma_u\,2\sigma_g)^6\,(2\sigma_u\,3\sigma_g\,3\sigma_u\,1\pi_g\,1\pi_u)^6\,(\text{PCOs})^1$
8	97 500	$(1\sigma_g\,1\sigma_u)^4\,(2\sigma_g\,3\sigma_g\,4\sigma_g\,2\sigma_u\,3\sigma_u\,1\pi_u\,1\pi_g)^9$
		$(1\sigma_g\,1\sigma_u)^4\,(2\sigma_g\,3\sigma_g\,4\sigma_g\,2\sigma_u\,3\sigma_u\,1\pi_u\,1\pi_g)^8\,(\text{PCOs})^1$

1s electrons were frozen in the $1\sigma_g$ and $1\sigma_u$ orbitals, and the remaining eight electrons were freely distributed among the $2\sigma_g$, $3\sigma_g$, $2\sigma_u$, $3\sigma_u$, $1\pi_u$ and $1\pi_g$ orbitals giving configurations which can be written $(1\sigma_g\,1\sigma_u)^4\,(2\sigma_g\,3\sigma_g\,2\sigma_u\,3\sigma_u\,1\pi_u\,1\pi_g)^8$. To treat C_2^- we added a PCO basis comprising 10s, 10p and 6d orbitals. In this subsection all results presented used PCO exponents generated using $\alpha_0 = 0.17$ and $\beta = 1.4$. The calculations presented here are for C_2^- in its equilibrium geometry for which $R = 2.396\ a_0$ (Huber and Herzberg 1979).

The previous MRMPS studies considered electron impact ionization of H_2 and H_3^+ (Gorfinkiel and Tennyson 2004, 2005), which are both two-electron systems. In this case the construction of ionized target plus PCO configurations is straightforward. This is not so here where there are many possible configurations that could be selected. The need to (a) get a good representation of the (pseudo)-continuum, (b) get good energies and wavefunctions for the physical states of the target, (c) obtain a balanced description between the target and scattering calculations and (d) keep the whole calculation computationally tractable meant that considerable experimentation was required. Table 1 summarizes the models, giving the target configurations used in (2), which were tested as part of the present study.

Besides choosing a basis set and a set of configurations, it is also necessary to build a set of target molecular orbitals. For standard scattering calculations these orbitals are normally ones associated with the N-electron target under consideration. However for calculations involving ionization the final target state only has $N - 1$ electrons; experience (Gorfinkiel and Tennyson 2004), echoed by tests performed as part of this work, has shown that use of orbitals associated with the ionized target gives best results. We therefore tested two sets of C_2 MOs, those generated from a self-consistent field (SCF) calculation and natural orbitals (NOs) generated using the prescription given previously (Halmová *et al* 2006).

Table 2 gives energies for states of C_2^- calculated with the various models and orbital sets. These can be compared with the results of our previous study (Halmová *et al* 2006) which, once nuclear motion effects had been taken into account, gave good agreement with the experimental results reported in Huber and Herzberg (1979).

We consider each model in turn. Model 1 gave reasonable target energies but the pseudo-state configurations are very limited as they are obtained from a single electron in a PCO and a frozen target C_2; this treatment is not consistent with the CAS-CI representation of C_2^-. Model 2 is more consistent in that eight electrons are frozen in all configurations. However this much more limited model gave poor energies for the target states; indeed with SCF MOs it did not even predict the correct ground state for C_2^-. Model 3 is built on model 2 but with only six target electrons completely frozen; it gives rather a large scattering Hamiltonian matrix and when tested did not give particularly good eigenphase sums. Model 4 was built as a hybrid between models 1 and 2 using the target configurations from the former and pseudo-state configurations from the latter. This model gave good target energies and a relatively small Hamiltonian matrix size for the scattering problem. This model formed the basis of our preliminary study

Table 2. C_2^- ground-state energies (negative numbers in E_h) and excitation energies (in eV) for different models and orbitals.

	$X\ ^2\Sigma_g^+$		$A\ ^2\Pi_u$		$B\ ^2\Sigma_u^+$	
Model	SCF MOs	C_2 NOs	SCF MOs	C_2 NOs	SCF MOs	C_2 NOs
1	−75.611 66	–	0.729	–	2.673	–
2	1.951	−75.537 09	−75.566 59	0.850	7.955	5.813
3	−75.594 80	−75.587 82	0.597	0.611	3.115	2.549
4	−75.609 56	−75.609 44	0.468	0.419	2.734	2.506
5	−75.626 75	–	0.883	–	2.717	–
6	−75.657 77	–	0.912	–	2.908	–
7	0.123	−75.714 19	−75.660 55	0.686	1.823	2.621
8	−75.720 75		0.689		2.621	
a		−75.672 13		0.557		2.355

[a] Previous calculations (Halmová *et al* 2006).

Table 3. Isotropic polarizabilities of C_2^- in a_0^3 for different models, orbitals and PCO basis determined by (α_0, β).

	$\alpha_0 = 0.17\,\beta = 1.4$		$\alpha_0 = 0.15\,\beta = 1.4$	$\alpha_0 = 0.17\,\beta = 1.5$	$\alpha_0 = 0.17\,\beta = 1.3$	
Model	SCF MOs	C_2 NOs	SCF MOs	SCF MOs	SCF MOs	C_2 NOs
1	26.42					
2	28.58	109.51				
3	67.49	12.24				
4	32.24		32.48	31.24	31.98	18.80
5	25.00					
6	24.55					

(Halmová and Tennyson 2008) and became our workhorse for test calculations. Model 5 is a slightly enlarged version of model 4 and behaves similarly.

Use of the partitioned *R*-matrix method allowed us to explore target models which implied significantly larger Hamiltonian matrices for the scattering problem. We therefore tested the effect of gradually expanding the CAS-CI used to generate the pseudo-states. The limit of the process is model 8, in which the same extended CAS is used in both parts of the calculation. However, its corresponding scattering model is far too big to be tractable (see table 4) and was not pursued. Our attempts to construct intermediate models, give numbers 6 and 7. Model 7 did not give good target energies. We therefore decided to concentrate on use of models 4, 5 and 6.

As can be seen from table 2, the use of C_2 SCF MOs gives results of similar quality to NOs, in contrast to more usual calculations where NOs give significantly better results. This is perhaps not surprising since the NOs were constructed to give a good representation of a range of electronically excited states of C_2, which is not our purpose here. The calculations reported below use SCF MOs unless otherwise stated.

There is one further target property which proved to be of considerable importance for the scattering calculations, that is the long-range polarizability of the C_2^- target. Gorfinkiel and Tennyson (2004) showed that the MRMPS method converges the long-range target polarizability in a way that standard close-coupling expansions do not. As is discussed below, a good representation of the polarizability is essential to get a good physical model of the electron–molecular anion collision as it provides the dominant attractive term in the interaction.

Table 3 shows the isotropic polarizabilities predicted by various of our target models. We could find no literature value for this parameter. Indeed it is not straightforward to calculate it with standard electronic structure codes, we tried, as they are not generally set up to treat molecular anions. The table shows that the calculated polarizability is generally stable with changes to the PCO basis but not with other aspects of the target model. In part this is because both excited states of C_2^- are dipole allowed from the ground state and low-lying. This makes the calculated polarizability particularly sensitive to the transition dipole and precise excitation energies of these states. Our results suggest that the true polarizabilty of C_2^- at $R = 2.396\ a_0$ is between 25 and 32 a_0^3, of this less than 10 a_0^3 arises from coupling to the two physical electronically excited states of C_2^-.

So far we have concentrated on our calculations of the physical properties of the target. There is however another property of importance for the scattering runs: the spectral coverage of the continuum by the pseudo-states. Figure 1 compares energy levels generated by various versions of model 4. The behaviour shown here, that the energy levels are stable to choice of PCO basis but very sensitive to the target model used, was also shown in the other comparisons we made (Halmová 2008). A common feature of all the comparisons is the sparsity of states directly above ionization. In principle one could get pseudo-states in this energy region by significantly expanding the *R*-matrix box size and the associated PCO basis; such a calculation was not deemed computationally tractable at present. However, as can be seen from the results presented below, our pseudo-state distributions lead to very small near-threshold electron impact detachment cross sections, which appears to be in agreement with the observations.

3.2. Scattering model

Test calculations using model 1 for *R*-matrix spheres of radius $a = 10\ a_0$ and 13 a_0 showed that $a = 10\ a_0$ gave stable results and this was used for all further calculations. COs were taken from Faure *et al* (2002) with the largest exponent functions removed. This basis contains functions with ℓ up to 4, i.e. g orbitals. Use of two different sets of PCOs were tested

$$4\text{-}14a_g\ 2\text{-}7b_{2u}\ 2\text{-}7b_{3u}\ 1\text{-}4b_{1g}\ 4\text{-}8b_{1u}\ 2\text{-}5b_{3g}\ 2\text{-}5b_{2g}\ 1a_u$$
$$4\text{-}24a_g\ 2\text{-}10b_{2u}\ 2\text{-}10b_{3u}\ 1\text{-}7b_{1g}\ 4\text{-}12b_{1u}\ 2\text{-}8b_{3g}\ 2\text{-}8b_{2g}\ 1a_u$$

in D_{2h} notation. The eigenphase calculated with the larger PCO set was slightly higher, so this was used for further calculation.

To go from the target models detailed above to the inner region *R*-matrix wavefunctions of (1) we followed the prescription developed previously (Tennyson 1996b) for standard *R*-matrix calculations. This prescription, which has been used successfully in many studies, is designed to provide a balanced treatment between the target, *N*-electron, and scattering, $N + 1$-electron problems. Table 4 details the configurations generated for the $N + 1$-electron calculations associated with each of the models described above. Also given is the size of the final Hamiltonian, a crucial parameter in determining the tractability of the calculation. Although our Hamiltonian construction algorithm is very efficient meaning the computational demands of this step of the calculation only depend weakly on the number of target states (and pseudo-states) included in the expansion (Tennyson 1996a), the diagonalization step still represents a major bottleneck.

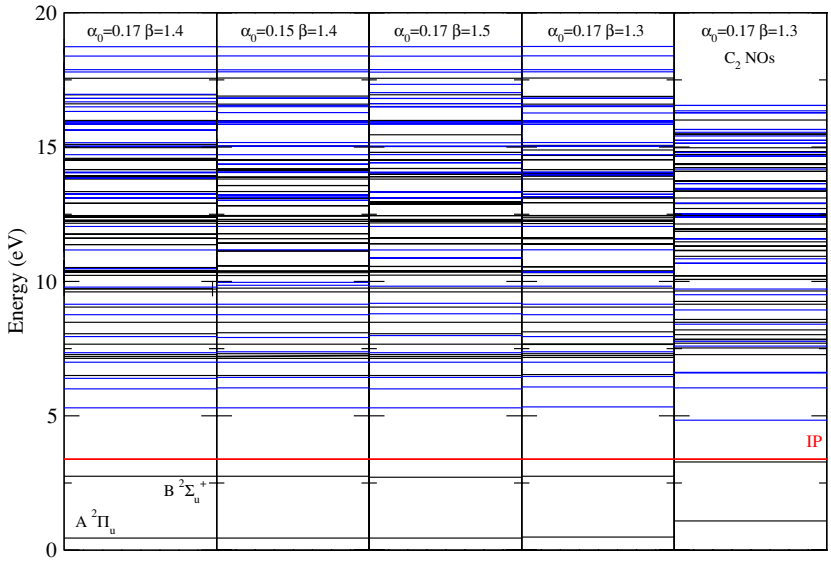

Figure 1. Target state distribution for C_2^- for model 4 for various (α_0, β) values as indicated in the figure. Energies are relative to the $X\,^3\Sigma_g^+$ ground state of C_2^-. SCF MOs of C_2 were used except where otherwise indicated. The horizontal line marked IP denotes the ionization threshold.

As a result, the largest previously published molecular R-matrix calculation was restricted to $N \sim 28\,000$ (Rozum *et al* 2003).

Model 8 gives an extremely large final step Hamiltonian and no attempt was made to actually solve for it. Many calculations were performed for models 1–6 for testing purposes. Calculations using the partitioned *R*-matrix method (Tennyson 2004) explicitly considered the lowest 1000 solutions which were found to be sufficient to span scattering energies up to about 40 eV.

Scattering calculations were performed for both singlet and triplet symmetries. After some experimentation it was decided to include 114 target states in the final close-coupling expansion. This number is evaluated in D_{2h} symmetry so counts states which are degenerate in $D_{\infty h}$ symmetry twice. Sixty-six of these states are doublets of which the lowest three are the physical states of C_2^-. The 48 quartet states only couple to triplet calculations. These states span energies up to about 19 eV above the target ground state for models 4, 5 and 6.

Outer region calculations were performed by propagating the *R*-matrices (Morgan 1984) to 100 a_0 and then matching to asymptotic Coulomb functions using a Gailitis expansion (Noble and Nesbet 1984). Since to our knowledge this was the first time the code had been used for a scattering problem involving repulsive Coulomb functions a number of simple test calculations were performed. Electron scattering from a frozen anionic target gave zero eigenphase sums as expected; these gradually got more structured as the scattering model improved. The large number of states included in the calculations presented here makes the outer calculations slow compared to standard *R*-matrix calculations. However we were still able to generate results for sufficient energies to map out the various resonance structures, both real and pseudo.

3.3. Born approximation

The interaction between the scattering electron and the C_2^- anion is long-range and repulsive. It can therefore be expected that many of the collisions will occur with a large impact parameter. Such collisions are not well represented in the calculations described above, all of which use a CO basis set and hence partial wave expansion truncated at $\ell = 4$. However, collisions with high values of electron angular momentum ($\ell > 4$) are amenable to a much simpler treatment since in these collisions the scattering electron can be assumed not to penetrate the charge cloud of the C_2^- target. Under these circumstances the collision cross sections are determined by purely long-range effects.

To allow the important effect of collisions with $\ell > 4$ in the inelastic cross sections presented here, we used a simple top-up procedure based on applying the Born approximation directly to the cross sections. This procedure was originally applied by Baluja *et al* (2001) and has recently been presented in some detail (Kaur *et al* 2008). There are a number of ways of applying such a Born top-up procedure but since C_2^- is non-polar, meaning rotational effects will be small, and the non-resonant cross sections at low ℓ are very small, meaning that interference effects for these ℓ's will not be important, the simplest procedure based on the direct augmentation of the cross sections was used. This procedure was applied to electron impact electronic excitation of all physical and pseudo-states which are dipole allowed, that is to all excitations to states of $^2\Sigma_u^+$ and $^2\Pi_u$ symmetry. Only transition dipole moments were considered for the long-range potential. For the pseudo-states these extra excitation cross sections were taken as supplementing the electron impact detachment cross sections. This increase turns out to be substantial showing that the majority of this process does in fact occur through long-range collisions.

Table 4. Configurations used for the various scattering models tested. N is the size of the resulting Hamiltonian matrix with ^1A_g symmetry and PCO means pseudo-continuum orbital and CO means continuum orbital.

Model	N	Configurations
1	21 705	$(1\sigma_g\ 1\sigma_u)^4\ (2\sigma_g\ 3\sigma_g\ 4\sigma_g\ 2\sigma_u\ 3\sigma_u\ 1\pi_u\ 1\pi_g)^9$ (COs)^1
		$(1\sigma_g\ 2\sigma_g\ 1\sigma_u\ 2\sigma_u\ 1\pi_u)^{12}$ (PCOs)^1 (COs)^1
		$(1\sigma_g\ 1\sigma_u)^4\ (2\sigma_g\ 3\sigma_g\ 4\sigma_g\ 2\sigma_u\ 3\sigma_u\ 1\pi_u\ 1\pi_g)^{10}$
		$(1\sigma_g\ 2\sigma_g\ 1\sigma_u\ 2\sigma_u\ 1\pi_u)^{12}$ (PCOs)^2
		$(1\sigma_g\ 2\sigma_g\ 1\sigma_u\ 2\sigma_u\ 1\pi_u)^{12}\ (3\sigma_g\ 4\sigma_g\ 3\sigma_u\ 1\pi_g)^1$ (PCOs)^1
2	6447	$(1\sigma_g\ 2\sigma_g\ 1\sigma_u\ 2\sigma_u)^8\ 1\pi_u^4\ (3\sigma_g\ 3\sigma_u\ 1\pi_g)^1$ (COs)^1
		$(1\sigma_g\ 2\sigma_g\ 1\sigma_u\ 2\sigma_u)^8\ 1\pi_u^3\ (3\sigma_g\ 3\sigma_u\ 1\pi_g)^2$ (COs)^1
		$(1\sigma_g\ 2\sigma_g\ 1\sigma_u\ 2\sigma_u)^8\ 1\pi_u^4$ (PCOs)^1 (COs)^1
		$(1\sigma_g\ 2\sigma_g\ 1\sigma_u\ 2\sigma_u)^8\ 1\pi_u^3\ (3\sigma_g\ 3\sigma_u\ 1\pi_g)^1$ (PCOs)^1 (COs)^1
		$(1\sigma_g\ 2\sigma_g\ 1\sigma_u\ 2\sigma_u)^8\ 1\pi_u^4\ (3\sigma_g\ 3\sigma_u\ 1\pi_g)^2$
		$(1\sigma_g\ 2\sigma_g\ 1\sigma_u\ 2\sigma_u)^8\ 1\pi_u^4\ (3\sigma_g\ 3\sigma_u\ 1\pi_g)^1$ (PCOs)^1
		$(1\sigma_g\ 2\sigma_g\ 1\sigma_u\ 2\sigma_u^8\ 1\pi_u^4$ (PCOs)^2
		$(1\sigma_g\ 2\sigma_g\ 1\sigma_u\ 2\sigma_u)^8\ 1\pi_u^3\ (3\sigma_g\ 3\sigma_u\ 1\pi_g)^2$ (PCOs)^1
		$(1\sigma_g\ 2\sigma_g\ 1\sigma_u\ 2\sigma_u)^8\ 1\pi_u^3\ (3\sigma_g\ 3\sigma_u\ 1\pi_g)^1$ (PCOs)^2
3	52 270	$(1\sigma_g\ 1\sigma_u\ 2\sigma_g)^6\ 1\pi_u^4\ (2\sigma_u\ 3\sigma_g\ 3\sigma_u\ 1\pi_g)^3$ (COs)^1
		$(1\sigma_g\ 1\sigma_u\ 2\sigma_g)^6\ 1\pi_u^3\ (2\sigma_u\ 3\sigma_g\ 3\sigma_u\ 1\pi_g)^4$ (COs)^1
		$(1\sigma_g\ 1\sigma_u\ 2\sigma_g)^6\ 1\pi_u^4\ (2\sigma_u\ 3\sigma_g\ 3\sigma_u\ 1\pi_g)^2$ (PCOs)^1 (COs)^1
		$(1\sigma_g\ 1\sigma_u\ 2\sigma_g)^6\ 1\pi_u^3\ (2\sigma_u\ 3\sigma_g\ 3\sigma_u\ 1\pi_g)^3$ (PCOs)^1 (COs)^1
		$(1\sigma_g\ 1\sigma_u\ 2\sigma_g)^6\ 1\pi_u^4\ (2\sigma_u\ 3\sigma_g\ 3\sigma_u\ 1\pi_g)^4$
		$(1\sigma_g\ 1\sigma_u\ 2\sigma_g)^6\ 1\pi_u^4\ (2\sigma_u\ 3\sigma_g\ 3\sigma_u\ 1\pi_g)^3$ (PCOs)^1
		$(1\sigma_g\ 1\sigma_u\ 2\sigma_g)^6\ 1\pi_u^4\ (2\sigma_u\ 3\sigma_g\ 3\sigma_u\ 1\pi_g)^2$ (PCOs)^2
		$(1\sigma_g\ 1\sigma_u\ 2\sigma_g)^6\ 1\pi_u^3\ (2\sigma_u\ 3\sigma_g\ 3\sigma_u\ 1\pi_g)^4$ (PCOs)^1
		$(1\sigma_g\ 1\sigma_u\ 2\sigma_g)^6\ 1\pi_u^3\ (2\sigma_u\ 3\sigma_g\ 3\sigma_u\ 1\pi_g)^3$ (PCOs)^2
4	6575	$(1\sigma_g\ 1\sigma_u)^4\ (2\sigma_g\ 3\sigma_g\ 2\sigma_u\ 3\sigma_u\ 1\pi_u\ 1\pi_g)^9$ (COs)^1
		$(1\sigma_g\ 2\sigma_g\ 1\sigma_u\ 2\sigma_u)^8\ 1\pi_u^4$ (PCOs)^1 (COs)^1
		$(1\sigma_g\ 2\sigma_g\ 1\sigma_u\ 2\sigma_u)^8\ 1\pi_u^3\ (3\sigma_g\ 3\sigma_u\ 1\pi_g)^1$ (PCOs)^1 (COs)^1
		$(1\sigma_g\ 1\sigma_u)^4\ (2\sigma_g\ 3\sigma_g\ 2\sigma_u\ 3\sigma_u\ 1\pi_u\ 1\pi_g)^{10}$
		$(1\sigma_g\ 2\sigma_g\ 1\sigma_u\ 2\sigma_u)^8\ 1\pi_u^4$ (PCOs)^2
		$(1\sigma_g\ 2\sigma_g\ 1\sigma_u\ 2\sigma_u)^8\ 1\pi_u^3\ (3\sigma_g\ 3\sigma_u\ 1\pi_g)^2$ (PCOs)^1
		$(1\sigma_g\ 2\sigma_g\ 1\sigma_u\ 2\sigma_u)^8\ 1\pi_u^3\ (3\sigma_g\ 3\sigma_u\ 1\pi_g)^1$ (PCOs)^2
5	12 283	$(1\sigma_g\ 1\sigma_u)^4\ (2\sigma_g\ 3\sigma_g\ 2\sigma_u\ 3\sigma_u\ 1\pi_u\ 1\pi_g)^9$ (COs)^1
		$(1\sigma_g\ 1\sigma_u)^4\ (2\sigma_g\ 2\sigma_u\ 1\pi_u)^8$ (PCOs)^1 (COs)^1
		$(1\sigma_g\ 1\sigma_u)^4\ (2\sigma_g\ 2\sigma_u\ 1\pi_u)^7\ (3\sigma_g\ 3\sigma_u\ 1\pi_g)^1$ (PCOs)^1 (COs)^1
		$(1\sigma_g\ 1\sigma_u)^4\ (2\sigma_g\ 3\sigma_g\ 2\sigma_u\ 3\sigma_u\ 1\pi_u\ 1\pi_g)^{10}$
		$(1\sigma_g\ 1\sigma_u)^4\ (2\sigma_g\ 2\sigma_u\ 1\pi_u)^8$ (PCOs)^2
		$(1\sigma_g\ 1\sigma_u)^4\ (2\sigma_g\ 2\sigma_u\ 1\pi_u)^7\ (3\sigma_g\ 3\sigma_u\ 1\pi_g)^2$ (PCOs)^1
		$(1\sigma_g\ 1\sigma_u)^4\ (2\sigma_g\ 2\sigma_u\ 1\pi_u)^7\ (3\sigma_g\ 3\sigma_u\ 1\pi_g)^1$ (PCOs)^2
6	12 283	$(1\sigma_g\ 1\sigma_u)^4\ (2\sigma_g\ 3\sigma_g\ 2\sigma_u\ 3\sigma_u\ 1\pi_u\ 1\pi_g)^9$ (COs)^1
		$(1\sigma_g\ 1\sigma_u)^4\ (2\sigma_g\ 2\sigma_u\ 1\pi_u)^8$ (PCOs)^1 (COs)^1
		$(1\sigma_g\ 1\sigma_u)^4\ (2\sigma_g\ 2\sigma_u\ 1\pi_u)^7\ (3\sigma_g\ 3\sigma_u\ 1\pi_g)^1$ (PCOs)^1 (COs)^1
		$(1\sigma_g\ 1\sigma_u)^4\ (2\sigma_g\ 2\sigma_u\ 1\pi_u)^6\ (3\sigma_g\ 3\sigma_u\ 1\pi_g)^2$ (PCOs)^1 (COs)^1
		$(1\sigma_g\ 1\sigma_u)^4\ (2\sigma_g\ 3\sigma_g\ 2\sigma_u\ 3\sigma_u\ 1\pi_u\ 1\pi_g)^{10}$
		$(1\sigma_g\ 1\sigma_u)^4\ (2\sigma_g\ 2\sigma_u\ 1\pi_u)^8$ (PCOs)^2
		$(1\sigma_g\ 1\sigma_u)^4\ (2\sigma_g\ 2\sigma_u\ 1\pi_u)^7\ (3\sigma_g\ 3\sigma_u\ 1\pi_g)^2$ (PCOs)^1
		$(1\sigma_g\ 1\sigma_u)^4\ (2\sigma_g\ 2\sigma_u\ 1\pi_u)^7\ (3\sigma_g\ 3\sigma_u\ 1\pi_g)^1$ (PCOs)^2
7	823 823	$(1\sigma_g\ 1\sigma_u\ 2\sigma_g)^6\ (2\sigma_u\ 3\sigma_g\ 3\sigma_u\ 1\pi_g\ 1\pi_u)^7$ (COs)^1
		$(1\sigma_g\ 1\sigma_u\ 2\sigma_g)^6\ (2\sigma_u\ 3\sigma_g\ 3\sigma_u\ 1\pi_g\ 1\pi_u)^6$ (PCOs)^1 (COs)^1
		$(1\sigma_g\ 1\sigma_u\ 2\sigma_g)^6\ (2\sigma_u\ 3\sigma_g\ 3\sigma_u\ 1\pi_g\ 1\pi_u)^8$
		$(1\sigma_g\ 1\sigma_u\ 2\sigma_g)^6\ (2\sigma_u\ 3\sigma_g\ 3\sigma_u\ 1\pi_g\ 1\pi_u)^7$ (PCOs)^1
		$(1\sigma_g\ 1\sigma_u\ 2\sigma_g)^6\ (2\sigma_u\ 3\sigma_g\ 3\sigma_u\ 1\pi_g\ 1\pi_u)^6$ (PCOs)^2
		$(1\sigma_g\ 1\sigma_u)^4\ (2\sigma_g\ 3\sigma_g\ 2\sigma_u\ 3\sigma_u\ 1\pi_u\ 1\pi_g)^{10}$
		$(1\sigma_g\ 1\sigma_u)^4\ (2\sigma_g\ 2\sigma_u\ 1\pi_u)^8$ (PCOs)^2
		$(1\sigma_g\ 1\sigma_u)^4\ (2\sigma_g\ 2\sigma_u\ 1\pi_u)^7\ (3\sigma_g\ 3\sigma_u\ 1\pi_g)^2$ (PCOs)^1
		$(1\sigma_g\ 1\sigma_u)^4\ (2\sigma_g\ 2\sigma_u\ 1\pi_u)^7\ (3\sigma_g\ 3\sigma_u\ 1\pi_g)^1$ (PCOs)^2
8	too big	$(1\sigma_g\ 1\sigma_u)^4\ (2\sigma_g\ 3\sigma_g\ 4\sigma_g\ 2\sigma_u\ 3\sigma_u\ 1\pi_u\ 1\pi_g)^9$ (COs)^1
		$(1\sigma_g\ 1\sigma_u)^4\ (2\sigma_g\ 3\sigma_g\ 4\sigma_g\ 2\sigma_u\ 3\sigma_u\ 1\pi_u\ 1\pi_g)^8$ (PCOs)^1 (COs)^1
		$(1\sigma_g\ 1\sigma_u)^4\ (2\sigma_g\ 3\sigma_g\ 4\sigma_g\ 2\sigma_u\ 3\sigma_u\ 1\pi_u\ 1\pi_g)^{10}$
		$(1\sigma_g\ 1\sigma_u)^4\ (2\sigma_g\ 3\sigma_g\ 4\sigma_g\ 2\sigma_u\ 3\sigma_u\ 1\pi_u\ 1\pi_g)^9$ (PCOs)^1
		$(1\sigma_g\ 1\sigma_u)^4\ (2\sigma_g\ 3\sigma_g\ 4\sigma_g\ 2\sigma_u\ 3\sigma_u\ 1\pi_u\ 1\pi_g)^8$ (PCOs)^2

We note that Ostrovsky and Taulbjerg (1996) developed a simple model of electron impact electron detachment from negative ions using a combination of the quantum tunnelling and classical field ionization. Their model is designed to

Table 5. Energy, E_r, and width, Γ, both in eV, of resonance states of C_2^{2-}; our results are based on calculations with $\alpha_0 = 0.17$ and $\beta = 1.4$.

	Previous work				Model 4		Model 5		Model 6	
Symmetry	E_r	Γ	Ref.	Symmetry	E_r	Γ	E_r	Γ	E_r	Γ
$^1\Sigma_g^+$	3.5	0.3	a	$^1\Sigma_g^+$	4.86	0.65	4.75	0.57	4.91	0.67
	10.0	2.1	b	$^1\Pi_g$	10.92	0.52	10.59	0.57	11.46	0.82
	10.0	3–4	b	$^3\Pi_g$	9.71	1.14	9.54	0.99	10.44	1.43

[a] Theory (Sommerfeld *et al* 2000).
[b] Experiment (Andersen *et al* 1996, Pedersen *et al* 1998, 1999).

reproduce the large impact parameter part of the cross section we compute using the Born approximation. It was considered by Pedersen *et al* (1999) for the case of a C_2^- target. Although this model is significantly different from our Born procedure both are designed to capture the essential physics of long-range collisions between charged particles.

4. Results

A very large number of different calculations was attempted. For space reasons only those performed using models 4, 5 and 6 will be reported in detail. As a major aim of this study was to characterize the resonances observed in the storage ring experiments, it is this aspect of the work we discuss first. We will then give our results for total cross sections for both electron impact electronic excitation and electron detachment.

4.1. Resonances

All models tested showed a $^1\Sigma_g^+$ resonance feature at about 5 eV. However only the more sophisticated models showed stable resonances in the energy region probed by the storage ring experiments.

Figure 2 gives a series of model 4 calculations for B_{3g} symmetry contribution to the total electron impact electron detachment cross section as a function of energy. Both singlet and triplet contributions are dominated by a series of resonance features: several narrow resonances which show a strong dependence on the PCO basis set parameters and a single broad resonance in each case. In contrast to the narrow resonances, the positions and widths of the broad resonance features are stable with respect to the choice of PCO basis; indeed even the calculation with $\alpha_0 = 0.17$ and $\beta = 1.5$ gives similar broad resonance features to the other calculations. This particular choice of PCO basis shows a significantly enhanced narrow resonance structure which is a known signature of a poorly converged PCO basis (Bray and Stelbovics 1992, Bartschat *et al* 1996). Figure 3 gives a similar comparison for the total electron impact detachment cross section where again both the singlet and triplet resonance features are clearly visible. The poorer quality of the calculation based on the use of C_2 NOs can clearly be seen.

Inspection of plots of eigenphase sums (not given) showed one further clear resonance at energies just above the ionization threshold of $^1\Sigma_g^+$ symmetry. Parameters for this resonance and those near 10 eV were obtained by fitting their eigenphases to

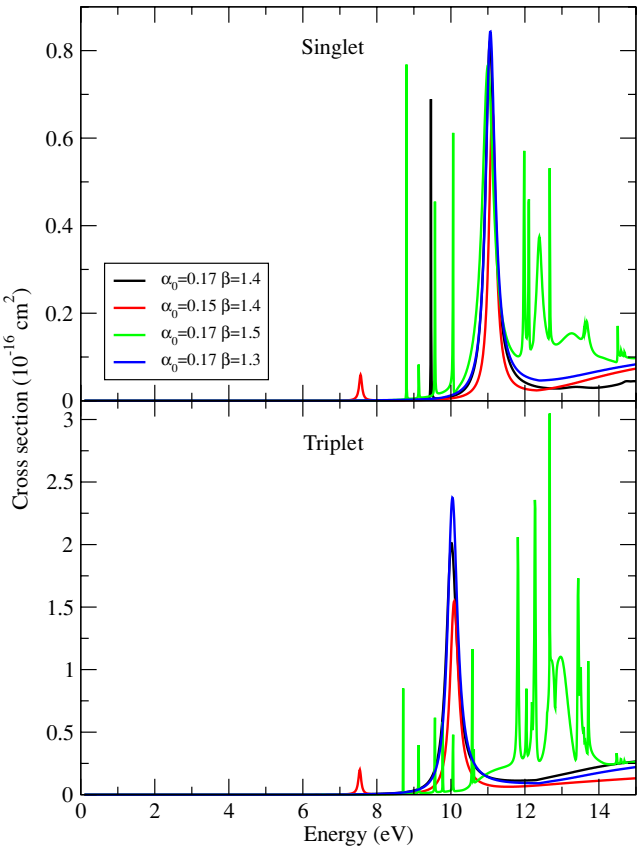

Figure 2. Partial electron impact detachment cross sections of C_2^- for model 4 for final states of B_{3g} (Π_g) total symmetry with different values of (α_0, β); ionization to singlet and triplet final states is shown to illustrate their distinct resonance structures.

a Breit–Wigner formula (Tennyson and Noble 1984). The resulting resonance parameters are given for model 4 in table 5, where they are compared to previous work.

Sommerfeld *et al* (2000) performed careful absorbing potential calculations on the closed shell $^1\Sigma_g^+$ resonance which lies close to the ionization threshold of C_2^-. We predict a similar resonance, albeit at slightly higher energy; this agreement can be considered satisfactory given the lower level of configuration interaction included in our study. This resonance occurs just above the electron detachment threshold where both our calculations and the observations suggest that the electron impact detachment cross sections are very small; neither show any obvious structure due to it. However we find two further resonances. These resonances lie close in energy to those detected experimentally (Andersen *et al* 1996, Pedersen

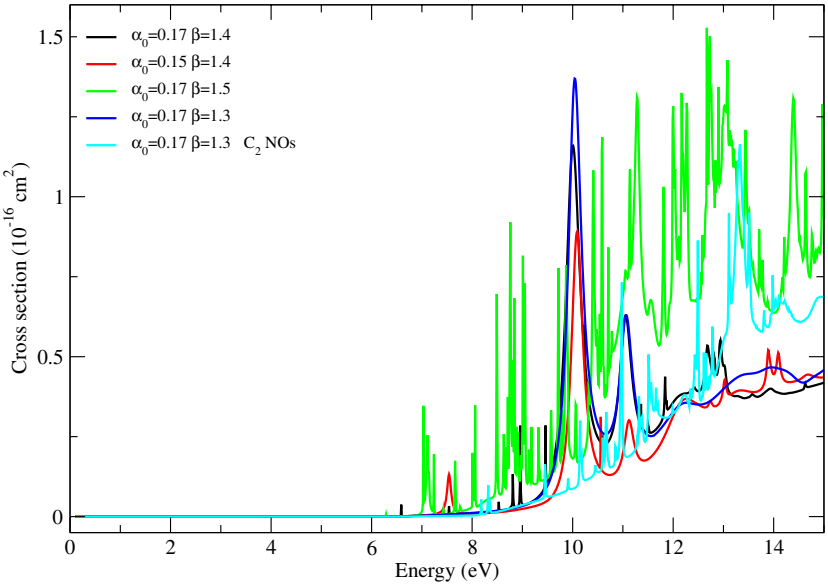

Figure 3. Total electron impact detachment cross sections of C_2^- for model 4 with different values of (α_0, β).

et al 1998, 1999). In fact the experiments give somewhat different resonance characteristics depending on whether they measure the detachment cross section, which gives a width of 2.1 eV, or the smaller dissociation cross section, which gives widths between 3 and 4 eV. However to really test whether these resonances agree it is necessary to make a more direct comparison with the experiments which means comparing with the measured cross sections.

4.2. Cross sections

Figure 4 gives a comparison between our calculations, performed with three different models, and the measurements. What is immediately apparent is that without the Born correction our cross sections are very significantly lower than the measured ones. This supports the assertion made above that the majority of the ionization occurs through large impact parameter collisions.

All the models shown give reasonable agreement with the measurements of Pedersen *et al* (1999). For completeness we give the measured results with and without consideration of simultaneous ionization and dissociation. Our calculations implicitly give the cross section for all processes that involve ionization and therefore should account for both channels. As the dissociation channel is relatively unfavoured, these two measurements are close together, the difference is certainly smaller than the accuracy of our calculations.

It can be seen that all three models give total ionization cross sections in good agreement with the measurements. In this context it should be noted that the cross sections should all go to zero below the ionization threshold which is at about 3.8 eV. Furthermore our resonance structures are very similar to, if a little higher in energy than, the observed ones. There are two reasons why we would expect our resonance energies to be a little too high. As discussed for the lower-lying $^1\Sigma_g^+$ resonance, our treatment of electron correlation effects (or short-range polarization) could be improved which would lead to a lowering of the resonance positions. Secondly our calculations ignore nuclear motion effects; inclusion of these should broaden the resonances somewhat and probably also lower their peak position. Given this, the agreement between our calculated and the observed resonance structures can be considered to be very good.

Finally figure 5 gives total electron impact electronic excitation cross sections for the two bound states of C_2^-. These excitations are both dipole allowed and the cross sections are again completely dominated by the high impact parameter, dipole-driven transitions which we characterize with the Born approximation. Again we use a simple Born correction to the total cross section. For the target states given by model 4 with C_2 SCF orbitals, as used for the results of figure 5, the absolute transition dipoles for X $^2\Sigma_g^+$–A $^2\Pi_u$ and X $^2\Sigma_g^+$–B $^2\Sigma_u^+$ are 1.02 D and 1.79 D respectively. These dipoles are significant but not huge; the larger than usual electronic excitation cross section found for X $^2\Sigma_g^+$–A $^2\Pi_u$ is a kinematic effect caused by the unusually low threshold found for this process. As we predict essentially no resonance structure in these electronic excitation cross sections, a simple Born calculation should suffice for this problem.

5. Discussion and conclusions

Our calculations detect the clear signature of three resonances: one of $^1\Sigma_g^+$ symmetry just above the ionization threshold and resonances with singlet and triplet spin and Π_g spatial symmetry at about 10 eV. Since they all lie above the excited electron states of C_2^-, these must be regarded as shape resonances. The standard model for shape resonances in electron–molecule collisions relies on a centrifugal barrier to provide the trapping potential. Such resonances have two characteristics: they are not found for s-wave scattering and they occur, often at too high an energy, in simple static exchange calculations. The present resonances are absent

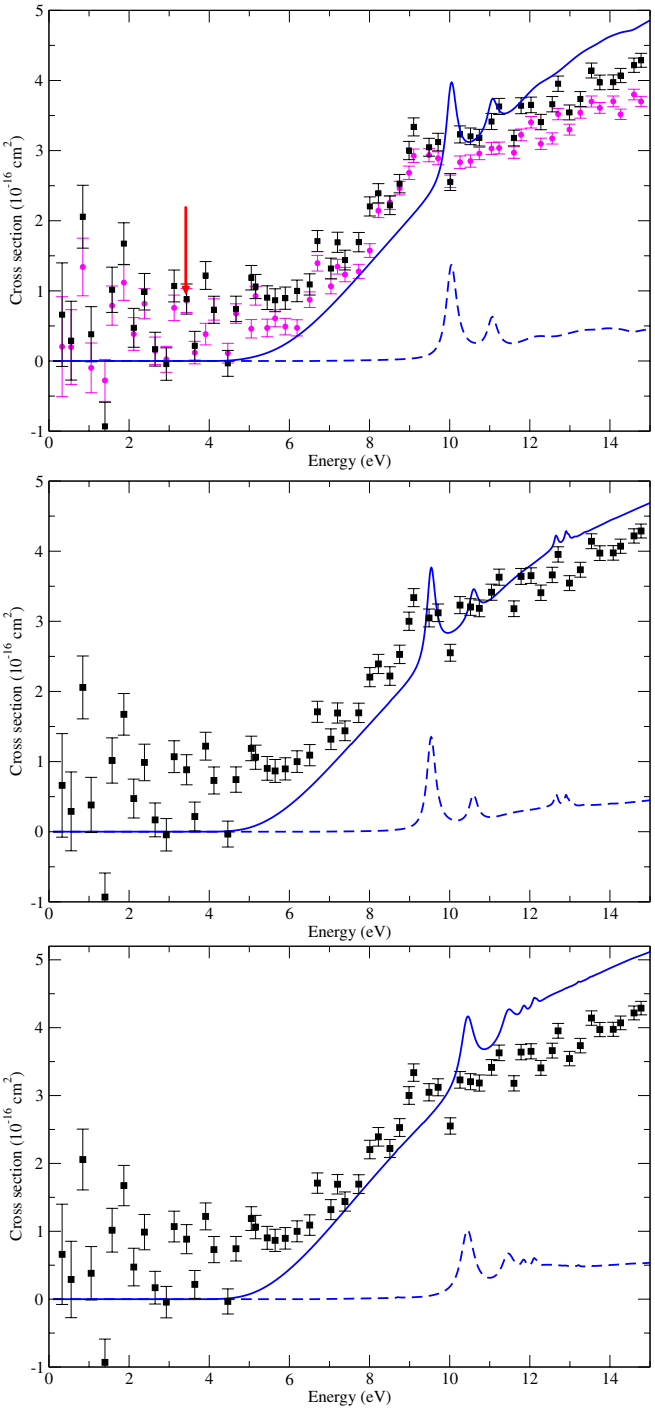

Figure 4. C_2^- electron impact ionization cross sections. Experimental data due to Pedersen *et al* (1999) are given by circles (without dissociative channels) and squares (with dissociative channels); the dashed lines represent our cross sections without Born correction; the solid lines represent our cross sections with Born correction. Top panel: model 4 with $\alpha_0 = 0.17$ and $\beta = 1.4$; middle panel: model 5 with $\alpha_0 = 0.17$ and $\beta = 1.4$; bottom panel: model 6 with $\alpha_0 = 0.17$ and $\beta = 1.3$.

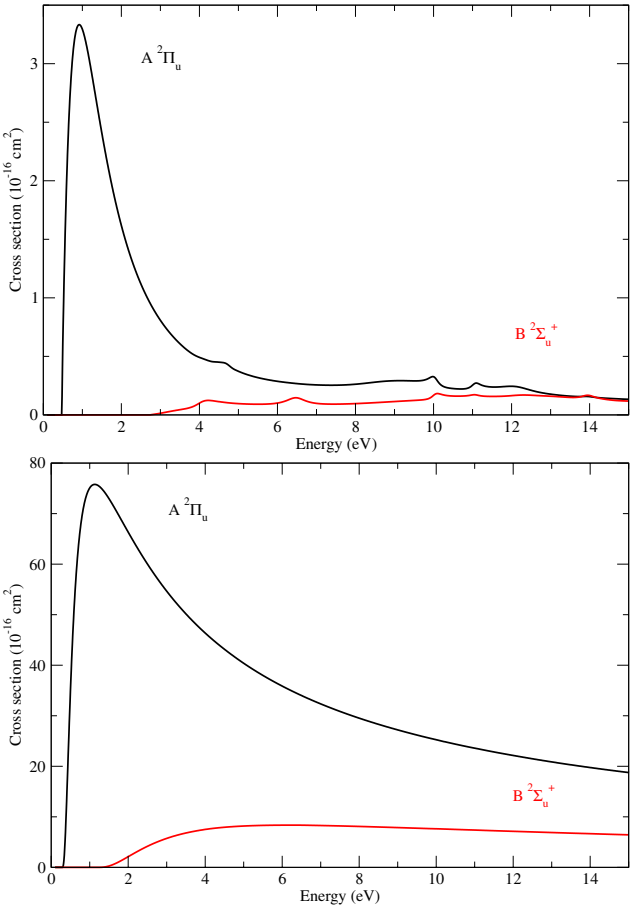

Figure 5. Electron impact electronic excitation cross sections for excitation to the A $^2\Pi_u$ and B $^2\Sigma_u^+$ states without (upper) and with (lower) Born correction; note the very different cross section scales for the two panels. Calculations are for model 4 with $\alpha_0 = 0.17$ and $\beta = 1.3$.

from the test static exchange calculations we ran and the $^1\Sigma_g^+$ resonance involves s-wave scattering.

All this implies a modified picture of a shape resonance. The situation here is that the scattering occurs under the influence of a strongly repulsive Coulomb potential. The well required to (temporarily) trap the scattering electron should therefore be the result of some local attraction. Our calculations suggest that this is indeed what happens and the attractive component is provided by polarization interactions. This is why characterizing the resonances requires such a sophisticated representation of the target wavefunctions.

Although representation of the resonances requires a very sophisticated treatment of the target, this is not the situation for the cross sections. Both the electron impact electronic excitation and electron detachment cross sections are dominated by long-range collisions which can be modelled using a simple Born approximation. It should however be noted that our treatment of the electron impact electron detachment process does involve the use of a discretized continuum via the MRMPS method which is then used to provide the necessary transition dipoles for the Born calculation.

In summary, our calculations on electron impact electron detachment of C_2^- reproduce both the resonance structure and cross sections observed over a number of years in storage rings (Andersen *et al* 1996, Pedersen *et al* 1998, 1999) for

this process. These calculations are the first to achieve either of these goals. To do this we had to combine a sophisticated treatment of the C_2^- target including representation of target continuum states using the molecular *R*-matrix with pseudo-states (MRMPS) method with a method for calculating the effects of high impact parameter collisions.

References

Andersen L H, Bak J, Boye S, Clausen M, Hovgaard M, Jensen M J, Lapierre A and Seiersen K 2001b *J. Chem. Phys.* **115** 3566

Andersen L H, Bilodeau R, Jensen M J, Nielsen S B, Safvan C P and Seiersen K 2001a *J. Chem. Phys.* **114** 147

Andersen L H, Hvelplund P, Kella D, Mokler P H, Pedersen B, Schmidt H T and Vejby-Christensen L 1996 *J. Phys. B: At. Mol. Opt. Phys.* **29** L643

Baluja K L, Mason N J, Morgan L A and Tennyson J 2001 *J. Phys. B: At. Mol. Opt. Phys.* **34** 2807–21

Bartschat K and Bray I 1996 *J. Phys. B: At. Mol. Opt. Phys.* **29** L577–83

Bartschat K, Hudson E T, Scott M P, Burke P G and Burke V M 1996 *J. Phys. B: At. Mol. Opt. Phys.* **29** 115–23

Bray I and Stelbovics A T 1992 *Phys. Rev. Lett.* **69** 53–6

Burke P G and Berrington K A (ed) 1993 *Atomic and Molecular Processes, an R-matrix Approach* (Bristol: Institute of Physics Publishing)

Burke P G and Tennyson J 2005 *Mol. Phys.* **103** 2537–48

Collins G F, *et al* 2005 *Phys. Rev.* A **72** 043708

Dunning T H 1970 *J. Chem. Phys.* **53** 2823

Faure A, Gorfinkiel J D, Morgan L A and Tennyson J 2002 *Comput. Phys. Commun.* **144** 224–41

Gorfinkiel J D and Tennyson J 2004 *J. Phys. B: At. Mol. Opt. Phys.* **37** L343–50

Gorfinkiel J D and Tennyson J 2005 *J. Phys. B: At. Mol. Opt. Phys.* **38** 1607–22

Halmová G 2008 *R*-matrix calculations of electron–molecule collisions with C_2 and C_2^- *PhD Thesis* University College London

Halmová G, Gorfinkel J D and Tennyson J 2006 *J. Phys. B: At. Mol. Opt. Phys.* **39** 2849–60

Halmová G and Tennyson J 2008 *Phys. Rev. Lett.* **100** 213202

Huber K P and Herzberg G (ed) 1979 *Constants of Diatomic Molecules* (Princeton, NJ: Van Nostrand-Reinhold)

Kaur S, Baluja K L and Tennyson J 2008 *Phys. Rev.* A **77** 032718

Morgan L A 1984 *Comput. Phys. Commun.* **31** 419–22

Morgan L A, Gillan C J, Tennyson J and Chen X 1997 *J. Phys. B: At. Mol. Opt. Phys.* **30** 4087–96

Noble C J and Nesbet R K 1984 *Comput. Phys. Commun.* **34** 399–411

Ostrovsky V N and Taulbjerg K 1996 *J. Phys. B: At. Mol. Opt. Phys.* **29** 2573–87

Pedersen H B, Djurić N, Jensen M J, Kella D, Safvan C P, Schmidt H T, Vejby-Christensen L and Andersen L H 1999 *Phys. Rev.* A **60** 2882–99

Pedersen H B, Djurić N, Jensen M J, Kella D, Safvan C P, Vejby-Christensen L and Andersen L H 1998 *Phys. Rev. Lett.* **81** 5302–5

Rozum I, Mason N J and Tennyson J 2003 *New J. Phys.* **5** 1–155

Schmidt M W and Ruedenberg K 1979 *J. Chem. Phys.* **71** 3951

Sommerfeld T, Riss U V, Meyer H D and Cederbaum L 1997 *Phys. Rev. Lett.* **79** 1237

Sommerfeld T, Tarantelli F, Meyer H D and Cederbaum L 2000 *J. Chem. Phys.* **112** 6635

Svendsen A, Bluhme H, El Ghazaly M A O, Seiersen K, Nielsen S B and Andersen L H 2005 *Phys. Rev. Lett.* **94** 223401

Tennyson J 1996a *J. Phys. B: At. Mol. Opt. Phys.* **29** 1817–28

Tennyson J 1996b *J. Phys. B: At. Mol. Opt. Phys.* **29** 6185–201

Tennyson J 1997 *Comput. Phys. Commun.* **100** 26–30

Tennyson J 2004 *J. Phys. B: At. Mol. Opt. Phys.* **37** 1061–71

Tennyson J and Halmová G 2007 *Mathematical and Computational Methods in R-matrix Theory (CCP2)* ed M Plummer *et al* (Warrington: Daresbury Laboratory) pp 85–90

Tennyson J and Morgan L A 1999 *Phil. Trans.* A **357** 1161–73

Tennyson J and Noble C J 1984 *Comput. Phys. Commun.* **33** 421–4